Actuated Electromagnetic System for Ice Removal

Kelly Allred, Jon Eble, Nicole Ela, Jacqueline Godina, Andre Litinsky,
Runnan Lou, Andrew Moorman, Elizabeth Thomas, and Colin Zohoori

2016 AIAA Conference

In an effort to provide a power efficient solution to the hazardous problem of in-flight icing on the wings of Unmanned Aerial Vehicles (UAVs), the undergraduate senior design team AESIR at the University of Colorado Boulder has researched, designed, and built an electromagnetic deicing mechanism. This mechanism is designed specifically to remove ice from a carbon fiber composite wing section. By operating on the principal of repulsive magnetic fields, this mechanism (consisting of a solenoid, target disk, and supporting circuitry) delivers an impulse of force acting on the wings interior leading edge causing an outward deflection of the surface and resulting in breakage and subsequent shedding of the ice. This impulse of force is provided by first using 570 V to charge a 500. F capacitor with 162 J of energy, and then followed by an operator-controlled capacitor discharge to allow for current flow through a 3-inch diameter solenoid. This discharge, over milliseconds, in conjunction with the aforementioned system parameters, delivers a 44.3 lb average impulsive force which, through modeling, is sufficient force (with a 30% margin) to remove a uniform 3/8 inch-thick layer of ice covering the leading edge of the wing.

Nomenclature

A	Magnetic potential
B	Magnetic field
d	Gap distance
F	Force
I	Current
J	Current density
L	Inductance
m	Mass
N	Number of wire loops
ω	Angular velocity
PE	Potential energy
R	Resistance
T	Torque
V	Voltage or Velocity

I. Introduction

Ice formation on aircraft during flight presents a critical problem as it is detrimental to flight characteristics and safety. Ice formation occurs when supercooled liquid droplets are present in cold atmospheric conditions; these super cooled droplets are capable of freezing to unprotected aircraft surfaces upon impact. As these droplets continue to freeze and accumulate on aircraft surfaces, the effects of the icing phenomena yield detrimental results for aircraft during flight. Specifically, the formation of ice on the leading edge of an aircraft's wings can cause a reduction in the overall lift-to-drag ratio $\left(\frac{L}{D}\right)$ resulting in an increased flight angle to maintain altitude as well as increased stall speeds.

In order to prevent these detrimental effects on high endurance unmanned aerial vehicles (UAVs), team AESIR has developed a solution using electromagnetism to deice the wings of a UAV. Extensive research in this field has shown that ice can be removed successfully through the rapid deflection of a surface on which the ice is adhered. This deflection is caused by an impulsive electromagnetic force impacting the wing's interior leading edge using a combination of high-voltage circuitry and magnetically-responsive materials. Using these guiding principles to form a baseline design, team AESIR has designed, built, and tested such a deicing mechanism with supporting circuitry for the application of UAV deicing.

With this problem statement and goal, the subsequent sections of this paper will review design objectives, design methodology, and design results of the developed system developed. The objectives as defined by the customer, Aurora Flight Sciences, hold the intention of integrating this deicing system with the high-endurance Orion UAV. To prove feasibility, team AESIR has calculated the force required to remove ice from the leading edge of the Orion UAV and in turn developed a model to determine the solenoid design required to produce the calculated force to remove the required amount of ice (3/8 inches). A deeper description of the methodology behind the development of the design is discussed later in this paper as well as methods used to verify the derived models through testing data.

II. Design Objectives

A. Levels of Success

Using customer requirements and design requirements, team AESIR has developed three levels of success to define this project. The first level of success involves the construction of a ballistic pendulum in which the solenoid will repel a metal target disk attached to a pendulum arm. This setup is used to calculate the force being produced by the actuator with various solenoid parameters and verifies the developed force model. Once the model has been verified and the properties of the solenoid are better understood, the deicing mechanism is implemented on a flat carbon fiber plate representative of the upper surface of the target wing section. The final level of success involves integrating the deicing mechanism with a test section that has the shape of the DAE11 airfoil to test for functionality in ice removal and structural model verification. This paper will focus on the force data obtained from the first level of success.

B. Requirements

In order to ensure the success of the project, the team developed four main requirements. These requirements were developed to ensure that the solution the team developed would meet the customers requirements as well as provide a functional deicing mechanism.

The first requirement is that the full-span system shall be integrable with the Orion UAV. This requirement ensures that the deicing mechanism can function within the Orion airfoil geometry as well as stay within the power requirement. The team will be verifying this requirement is met through analysis of the testing data as well as using visual inspection to verify the mechanism fits in the wing section. The second requirement states that the deicing mechanism shall remove ice. This requirement was derived to meet the customers requirement as removing ice is the main purpose of the project. The team will be verifying this requirement through demonstration. The deicing mechanism will be tested under icing conditions to certify it can remove ice off of the surface of the wing. The last requirement is that the full-span system shall use less than 4kW-hr of energy to deice the wing section; this once again is a customer requirement. As the Orion UAV has a long mission, the unmanned aircraft has limited power to deice a wing should icing conditions occur. To verify this requirement, the team will has conducted level one testing and analysis as described in further sections. For this testing, the team used a power supply and multimeter to indicate the voltage being supplied to the system as well as further analysis to determine power consumption for the full wingspan.

These aforementioned requirements provide guidelines for designing and building the deicing mechanism. Meeting these requirements will guarantee that the team has not only designed, built, and tested a deicing mechanism, but also provided Aurora Flight Sciences with level 1 test data that can be used to understand and optimize the system.

III. Design Methodology

A. Design Description

1. Electromagnetic Deicing Mechanism

To satisfy the previously discussed requirements, the team conducted a trade study which factored in energy usage, weight, cost, technology readiness level, difficulty, and complexity. From this trade study, it was determined that electro-impulse deicing was the best solution to meet the design requirements. Electro-impulse deicing works by converting energy in the form of electricity flow into a magnetic field and then into a subsequent force. At a high level, the series of events starts by passing a current through a coiled wire (solenoid); the changing current generates a changing magnetic field. As the magnetic field increases, eddy currents are induced in a metal plate (target disk) located directly above the coil separated by a gap distance (see Fig. (1)). These eddy currents generate a second magnetic field with similar direction to the first field. Due to the similar magnetic field directions, the fields repel each other generating an impulsive force; this force acts equally and oppositely on the solenoid and the metal plate. With a

target disk attached to the interior leading edge of the wing and the solenoid supported just beneath the target disk, it is this repulsive force between the two components which causes a rapid deflection of the wing's surface causing the ice to crack and break off of the wing.

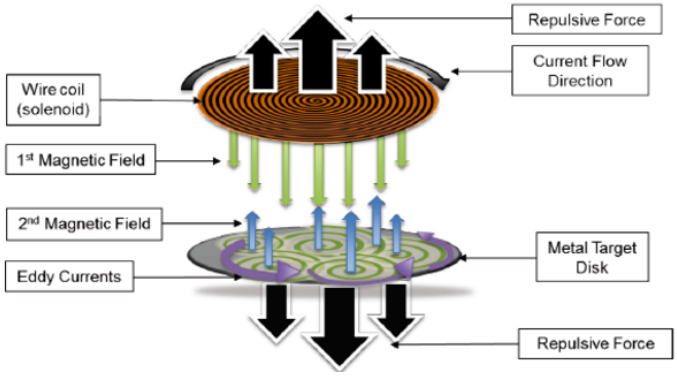

Figure 1: Electromagnetic deicing system theory diagram.

For testing of the electro-impulse deicing, the team used the following circuit. This consists of a 1000 V power supply, a 500 uF capacitor, a copper magnet ribbon wire spiral solenoid, and multiple thyristors (SCRs) for control of charging and discharging the capacitor. This schematic is visible in Fig. (2).

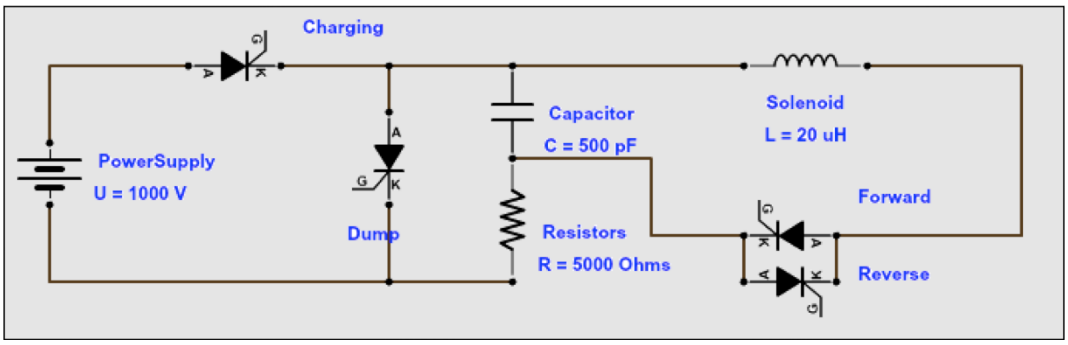

Figure 2: Electromagnetic Deicing System Schematic.

2. *Mechanism Integration with Representative Wing*

To satisfy ice removal requirements, the deicing mechanism has been integrated with a representative wing section; i.e. a carbon fiber flat plate containing dimensions and a honeycomb core analogous to the wing of the Orion. Using the simple shape of a flat plate allows the material and ice properties to be empirically checked without the complexity of a curved wing section, which could introduce error.

For a more realistic integration of this mechanism with the shape of a wing, there are several options available. One of these options, as developed by team AESIR through extensive research, includes a housing unit to hold the solenoid a gap distance from the target disk as well as a support structure to attach the housing unit to the spar as shown in Fig. (3).

To minimize payload mass to the UAV, the housing unit consists of two thin plates made of polyethylene which connect together via nylon screws and nylon nuts. The solenoid sits partly in the base plate with an extruded cylinder out of the top plate to decrease the gap distance between the solenoid and the target disk while accounting for the curvature of the wing. This housing unit assembly rests in an extruded cut of two carbon fiber foam composite plates sitting symmetrically beneath the housing unit and attached to the housing unit via corner braces. The polyethylene, nylon, and composite materials were chosen due to their non-metallic nature and hence no interference with the electromagnetic fields being generated by the solenoid (as this would result in losses and lower efficiency). Even though the above Fig.displays a representative wooden spar, the carbon fiber can be trivially attached to any spar either during layup for a composite spar, or with additional corner braces for a more ductile, non-composite spar. Regardless

of the integration chosen with this mechanism, the two most critical factors to consider are material selection and geometry with the desired wing.

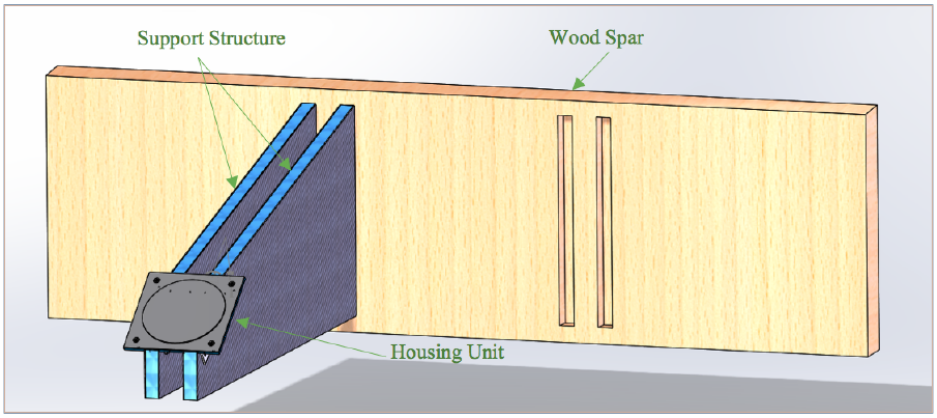

Figure 3: Housing unit and support structure assembly.

Finally, for the electromagnetic force to impact the leading edge, the target disk is adhered to the wings interior, however this is only a temporary solution for testing. For full-wing integration, the target disk can be laid up between carbon fiber pre-impregnated layers. Because the force between the target disk and solenoid is repulsive, the disk is being pushed into the material and hence will not de-laminate the composite layers upon impact. Should the wing be comprised of a metal, the wing's surface can simply act as a target disk and thus the system would not require an additional target disk.

B. Model Development from Driving Requirements

With this electromagnetic deicing mechanism and associated integration structures designed to meet both functional and design requirements, team AESIR developed the following models to verify and validate this design against its requirements. These models begin with knowing the force needed to break the required thickness of ice (inches) off of the representative carbon fiber wing section (i.e. flat plate). In the following model, the solenoid force model, the solenoid, target disk, and circuitry parameters are then used in conjunction with a range of voltages to show which voltage can provide the force required to break the ice per the first model.

1. ANSYS Ice Rupture Force Model

To determine the force required to break ice (i.e. achieve a stress in the representative ice layer that is greater than the ultimate tensile strength of the ice), AESIR created the following ANSYS model using the representative carbon fiber flat plate. For each iteration of modeling, a different pressure was applied to the target disk to find the minimum force required to achieve ultimate tensile strength of the ice, 347 psi. This ultimate tensile strength was determined from a combination of research [1] and preliminary testing data conducted to determine the accuracy in the researched value. Upon running model simulations, this minimum force value was found to be 44.3 lbf; this trial, along with the other simulations, is shown in Fig. (4).

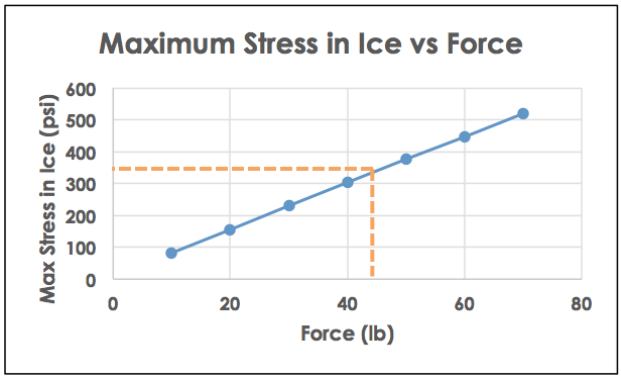

Figure 4: Maximum stress in ice vs. force for flat plate with 3/8 inches thick ice.

2. *Solenoid Force Model*

To explore the design space and optimize the deicing mechanism a solenoid force model was developed. This model was developed using Maxwells Equations in conjunction with Faradays Law and Lorentz's Force Law. In essence, the inductance of the wire coil changes the rate of change of current. Eq. (1) [2] shows the inductance approximation for a spiral coil inductor (solenoid). Eq. (2) [2] describes the relation of current based on inductance; the change in current generates and changes the magnetic field over time.

$$L = \frac{(N * \frac{1}{2}D_0)^2}{4D_0 + 11(D_0 - D_i)} \tag{1}$$

$$I(t) = \frac{V_s}{R}(1 - e^{\frac{-Rt}{L}}) \tag{2}$$

Maxwells equation, shown in Eq. (3) [3] relates the electrical field intensity, (E), to the magnetic flux density (B). The change in the B field is caused by the change in current over time. The parameters of the design may be modeled using external current density, Je, and the Eq. of B as related to the magnetic potential, A; see Eq. (4) and Eq. (5) [3].

$$\nabla \times E = \frac{-\partial \mathbf{B}}{\partial t} \tag{3}$$

$$\sigma \frac{\partial A}{\partial t} + \nabla \times \left(\mu_0^{-1}\mu_r^{-1}\nabla \times A\right) = J_e \tag{4}$$

$$B = \nabla \times A \tag{5}$$

Furthermore, the current density and the magnetic field are related by the torque created (see Eq. (6) [3]). In Eq. (6) describes the point at which the torque is measured while J and B are the current density and magnetic field. Using Lorenzs force, the torque may be used to find the force created as seen in Eq. (7) [3].

$$T = \int_V r \times (J \times B)\, dv \tag{6}$$

$$F = \int_{\partial\Omega} T\hat{n} dS \tag{7}$$

Starting with the design parameters and the following equations the force produced by the design may be determined. In essence, though, the design is governed by material properties, Maxwells equations, and Lorenzs force. The model can vary the following parameters. Based on this model the following force versus voltage plot was calculated with the following input parameters.

Input Parameters

- I – Current
- N – Number of wire loops
- H – Height
- D – Diameters
- d – Gap distance
- σ – Electric conductivity
- μ – Magnetic permeability

Figure 5: Model input parameters

Copper Solenoid Parameter	Value
Outer diameter	3.000 in
Inner diameter	0.039 in
Height	0.190 in
Wire thickness	0.030 in
Average gap between wire loops	0.007 in
Number of turns	36

Figure 6: Modeled Solenoid Properties

Copper Target Disk Parameter	Value
Gap distance	0.078 in
Disk thickness	0.078 in
Disk Diameter	4.000 in

Figure 7: Modeled Solenoid Properties

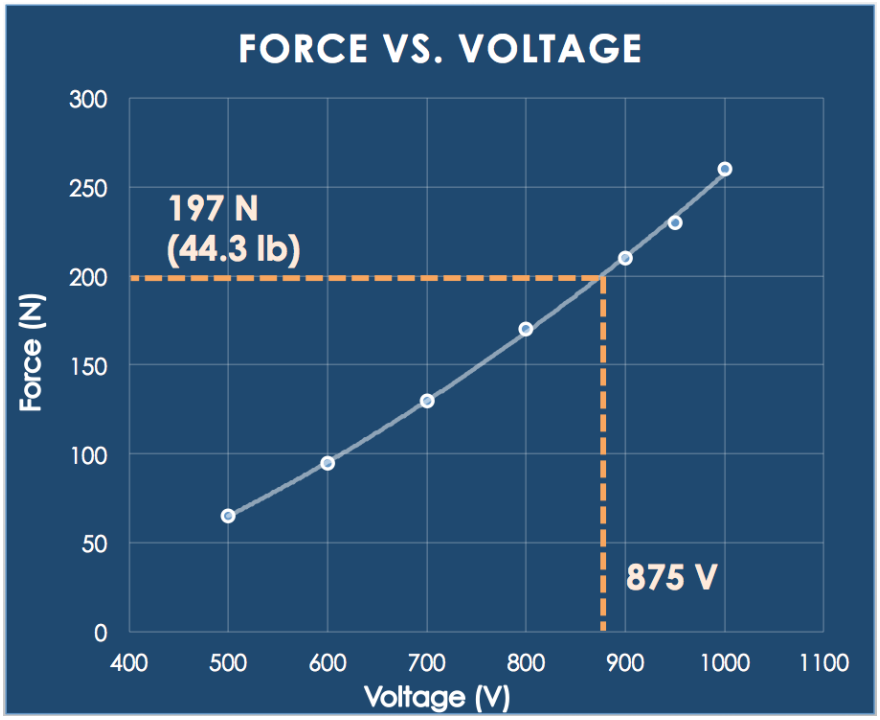

Figure 8: Solenoid force model for 3 inch solenoid.

From this it is seen the force that was required to break ice (44.3 lbf) can be achieved at about 875 V. In addition, with all circuitry components rated for 1000 V, this provides a 40% margin should the need for a higher force to achieve deicing be required.

IV. Design Results

Testing was completed to determine if the designed solenoids produce the predicted amount of force. There are a large range of variables in finding the magnetic force so empirical trends help to clarify the impact of some of the most critical variables for this problem. Specifically studied here were the number of turns to be fit within a set geometry and the amount of voltage to which the capacitor is charged (and therefore discharged). Knowing these parameters helps determine desirable configurations and the power required for a force produced.

A. Ballistic Pendulum Testing

To determine the force produced by the solenoid a ballistic pendulum was used, placing the target disk on the end of the pendulum so that the force produced by opposing magnetic fields swings the pendulum arm. For the test data to yield good results, the components of the ballistic pendulum were carefully designed and manufactured to minimize losses. The white pendulum arm shown in Fig. (9) was constructed in a Y-shape configuration to eliminate yawing and rolling motions that would contribute to losses in pitching. Additionally, the pendulum arm was made from nylon to ensure there was no leakage in Eddy currents from the mounted target disk. Purchased, well-lubricated pillow bearings were paired with a $\frac{3}{8}in.$ steel rod to ensure negligible loss in rotational friction. Excepting the pillow bearings and the rod, the pendulum components were manufactured at the University of Colorado Boulders Aerospace Instrumentation Shop. The pendulum frame was constructed using wood with the pendulum arm and solenoid housing block were machined from nylon.

The pendulum dynamics were used to find the impulse and average force applied based on the angle to which the arm rotates. The pendulum rotation is based on the force which occurs in the solenoid so the rotation varies with voltage applied and the solenoid design. The angle is determined by an in-house encoder which is made up of a high-speed camera recording at 600 fps and a 360 protractor mounted on the axis of rotation. Recordings capture the rotation of the pendulum arm. This set-up is show in Fig.(9).

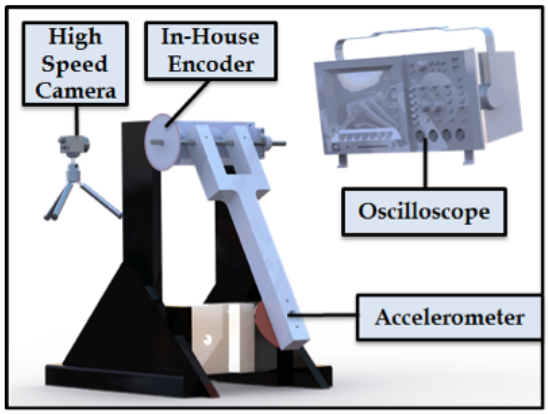

Figure 9: Ballistic pendulum test setup.

Assuming the only forces acting on the system are the magnetic force and gravity, conservation of energy and impulse equations were used to analyze the degree of pendulum rotation to find impulse applied. Note: this assumes all the magnetic force was confined to a single-axis pitching motion. If all the energy added to the system was transformed into potential energy when the pendulum reaches its max rotation, Eq. (8) may be used to find the potential energy.

$$PE = mgh = mg[Lcom * (1 - \cos\theta)] \tag{8}$$

This potential energy was equal to the energy in the pendulum system immediately after the impulse is applied (using the aforementioned assumptions). Knowing the energy just following the impulse, and assuming the force acts perpendicular to the pendulum arm, the angular velocity at the impulse location (Eq. (9) was found and then the velocity of the center of mass (Eq. (10)).

$$\omega = \sqrt{\frac{2 * PE}{I}} \tag{9}$$

$$V = \omega \times r \tag{10}$$

The principle of impulse shown in Eq. (11) was then used to determine the impulse.

$$Im = V * m \tag{11}$$

One important point to note is that this assumes the entire impulse occurs prior to the pendulum beginning to move. This is a reasonable assumption because the capacitor discharge occurs in 5.3 or 1.9 sec (depending on which solenoid in Table (1) is used); however this along with the other assumptions introduced error into the calculation. The tested solenoid parameters appear in Table (1). Note that for each solenoid different gap distances are tested. Solenoid 1 was tested at a 4 mm gap while Solenoid 2 was at a 7 mm gap.

Solenoid	Outer Diameter	Inner Diameter	Number of Turns
1	3 in	0.25 in	60
2	3 in	0.25 in	36

Table 1: Solenoid Parameters For Testing.

Using the data from testing solenoids 1 and 2 at series of voltages results in the impulse and average force trends shown in Fig. (10), Fig. (11), Fig. (12), Fig. (13).

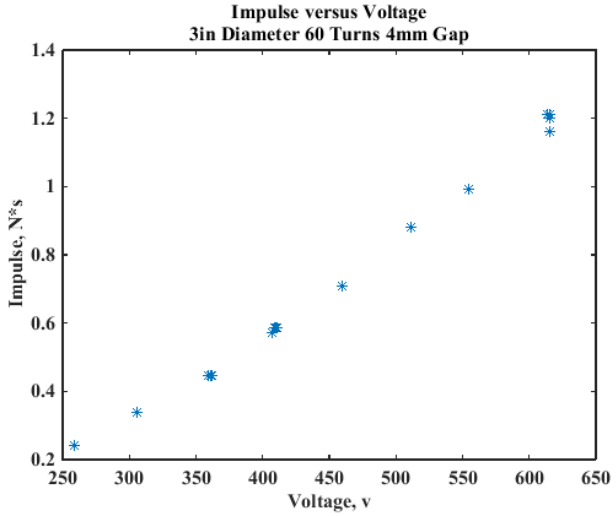

Figure 10: Impulse results for solenoid 1 with varied voltage.

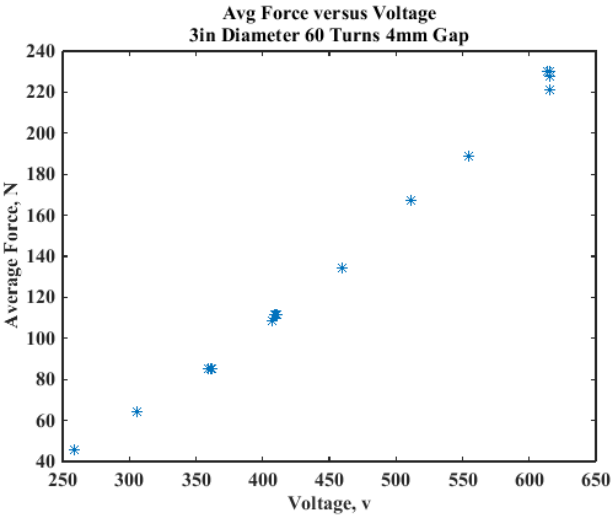

Figure 11: Average force results for solenoid 1 with varied voltage.

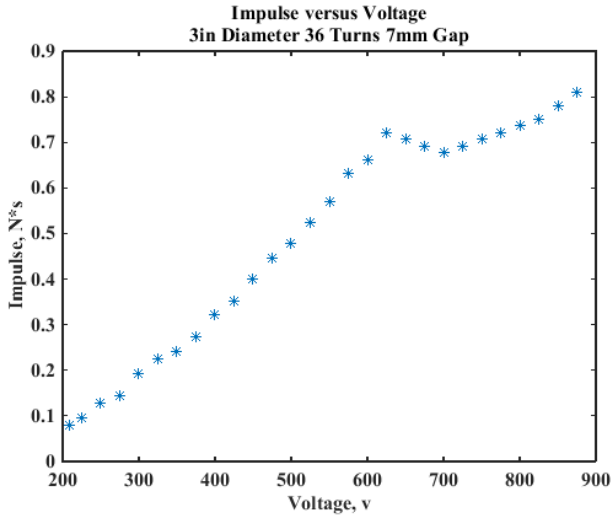

Figure 12: Impulse results for solenoid 2 with varied voltage.

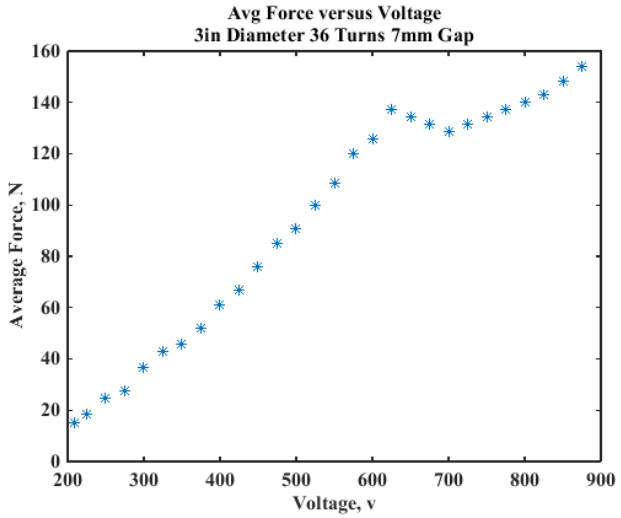

Figure 13: Average force results for solenoid 2 with varied voltage.

From these results it is evident that the geometry of the solenoid is critical to obtaining sufficient force. The higher number of turns and lessened gap distance yield about a 33% increase in average force. The second solenoid, at the tested voltages, cannot produce the force required to break the ice; however, fitting the data to a linear trend line, yields the required 197 N when the capacitor is discharged at 570 V. This equates 81.2 J stored on the capacitor, and 162.5 J total required to charge the capacitor. Each solenoid will be placed approximately 2-3 ft apart, which means deicing can be accomplished for about 80 J per foot at any supply power. Supply power only affects how long the deicing cycle would take.

Between the data sets for Solenoid 1 and 2, a linear trend fits best with both sets, but Solenoid 2 results do contain an unexpected increase and subsequent drop in impulse imparted between 600 and 700 V. To determine if this is anomalous further testing will be required.

The best fit trend matches with the predicted trend of voltage increase resulting in a linear increase in average force produced by the solenoid. The overall product, however, under preforms when compared to the modelled voltage versus average force. This is due to the assumptions made in the model. First and foremost is that the model assumes an air-filled gap between each wire loop in the solenoid coil. In reality, this gap size is not as regular so potentially some coils have a larger or smaller gap distance. Changing the gap between wires has complex effects so the modeled

and manufactured solenoids differ significantly. In addition, this model assumes the pendulum arm acts as a point mass acting at the center of mass for the system.

V. Conclusion

The electromagnetic force deicing system has the potential to be a power efficient method of removing ice following some refinement in the modeling and design. The impulse is controllable by the amount of voltage to which the capacitor is charged, meaning the system can be tailored to a variety of applications. For the immediate application here, removing ice from a UAV's leading edge, the electromagnetic system produces the required amount of force, being 44.3 lbf. In addition, the modeling accurately predicts the trend of the impulse but contains error in the assumptions it makes about the solenoid geometry and wire spacing. Future work for the project is to better categorize this discrepancy so that the impulse may be better predicted depending on the solenoid design. To complete this, more extensive data is being taken on the trends between parameters such as gap distance between the solenoid and target plate as well as the effect of diameter and turns within the given diameter. Should these trends continue to match the predicted trends but at reduced average force, the model outputs may be adjusted by a "manufacturing error" factor. Upon completion, the force generation method will be viable for multiple applications.

References

[1] Sammonds, P. R., and M. A. Rist. Ice-Structure Interaction.Strength and Failure Modes of Pure Ice and Multi-Year Sea Ice Under Triaxial Loading. By S. A. F. Murrel. N.p.: n.p., n.d. N. pag. Print.

[2] Adhesives and Applicators. Dragon Plate. N.p., n.d. Web. https://dragonplate.com/ecart/cartView.asp?rp=product

[3] Scherz, Paul, and Simon Monk. 3.7 Inductors.Practical Electronics for Inventors. 3rd ed. New York:McGraw-Hill, 2013. 355-374. Print.

[4] Dragon Plate: Material Specifications.Carbon Fiber PP Honeycomb Core(n.d.): n. pag. Dragon Plate. Web.http://dragonplate.com/docs/DPSpecPP-Honeycomb.pdf.